

Anisotropies in the flux of ultra-high energy cosmic rays

Edivaldo Moura Santos ^{1,2}
for the Pierre Auger Collaboration

¹ Instituto de Física, Universidade de São Paulo (USP)

² Department of Astronomy and Astrophysics, University of Chicago

4th CRA 2017, 10-13 October, Guadalajara, Jalisco, México

Overview

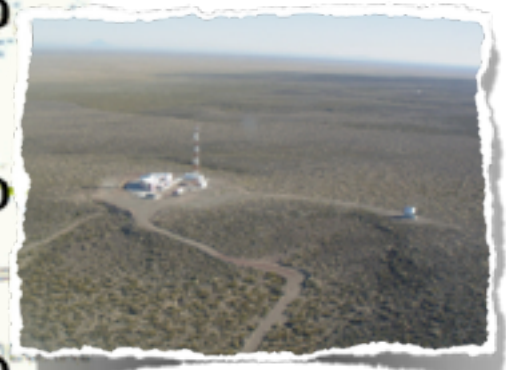
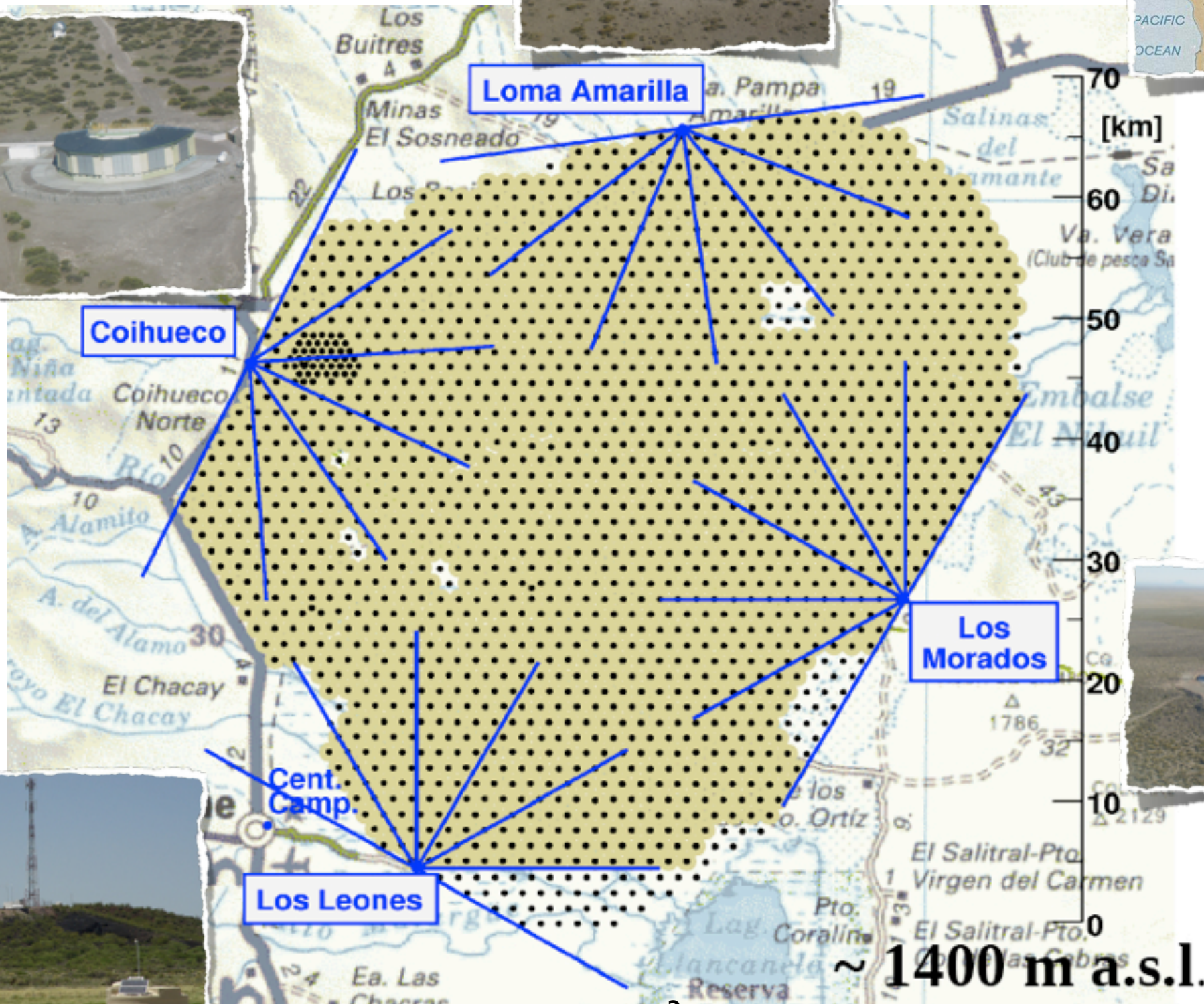
- **Some notes on datasets**
- **Searches for small to intermediate scale anisotropies**
- **Searches for large scale anisotropies**
- **Combined full sky analyses**
- **Summary**

The Pierre Auger Observatory

3000 km² surface array (1660 detectors)

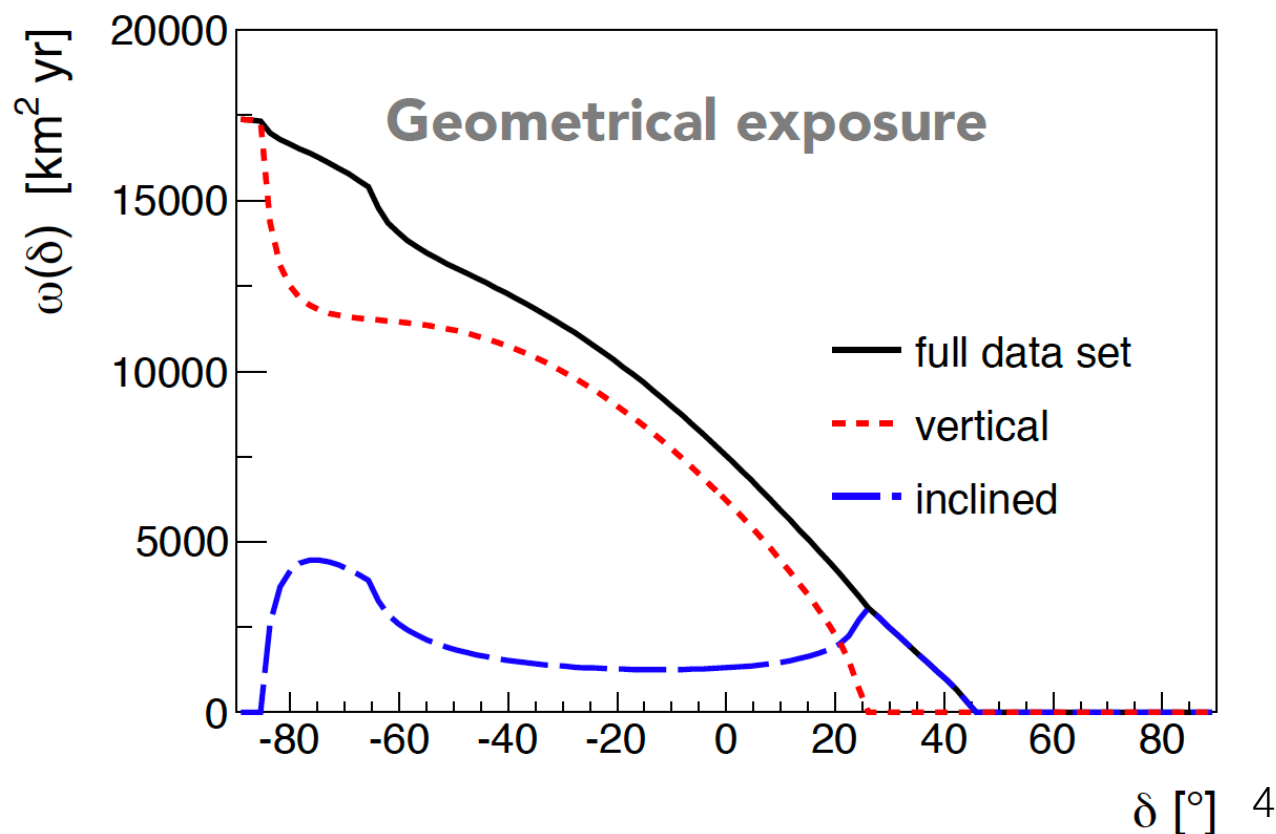
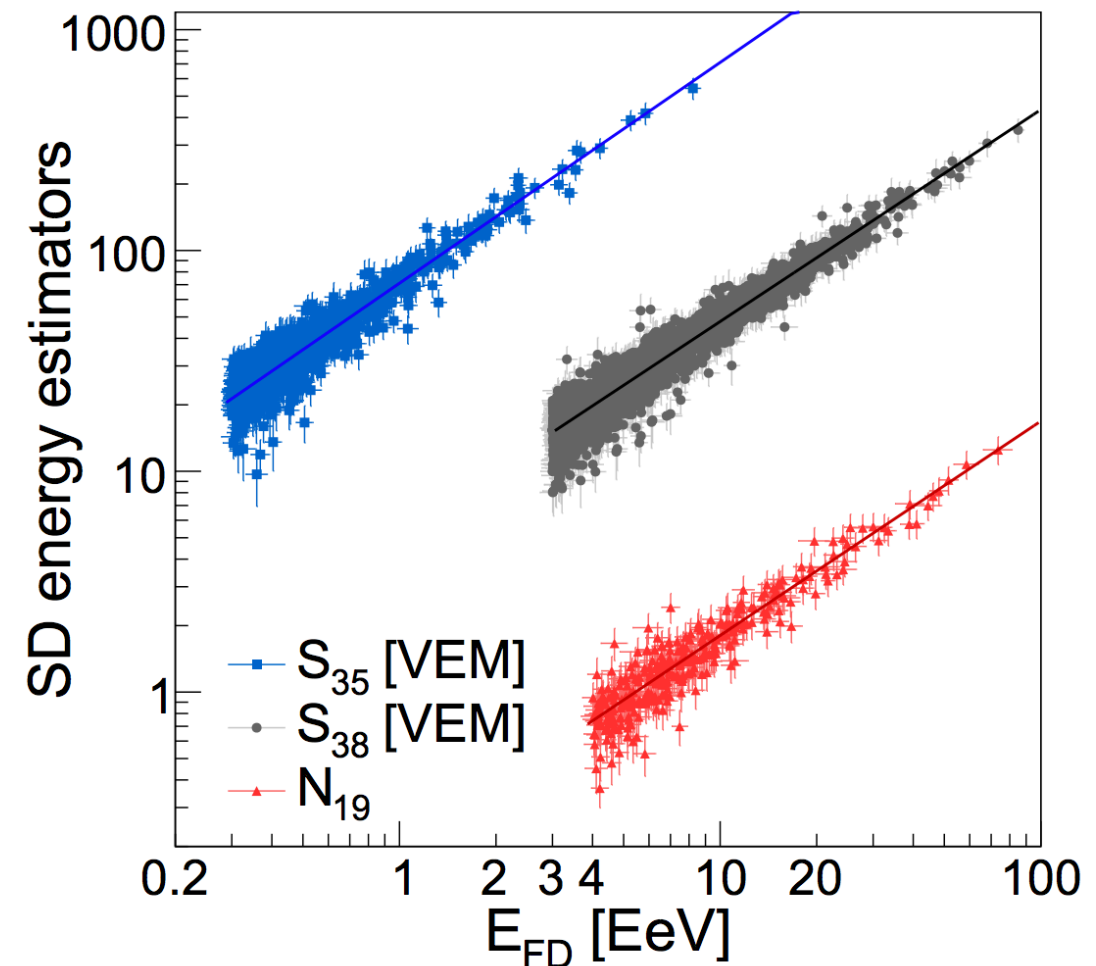
1.5 km triangular grid

27 fluorescence telescopes



General note on Auger SD data samples - I

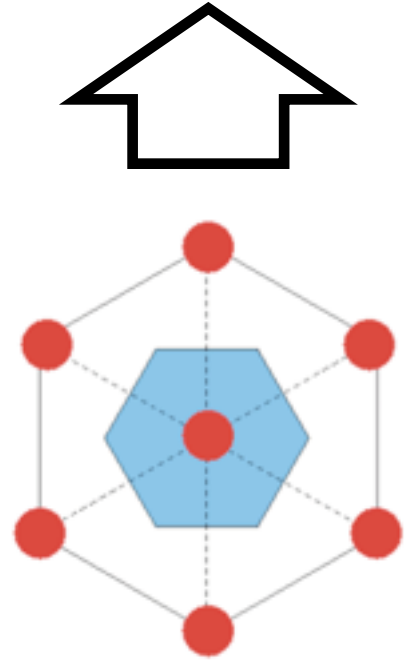
- Data-driven energy calib. using hybrid events
- Different SD estimators are correlated to the quasi-calorimetric energy measured by the FD
- Here, we should use two samples, depending on the zenith angle of the events:
 - **Vertical:** $0^\circ < \theta < 60^\circ$ ($S_{38} \times E_{FD}$)
 - **Inclined:** $60^\circ < \theta < 80^\circ$ ($N_{19} \times E_{FD}$)



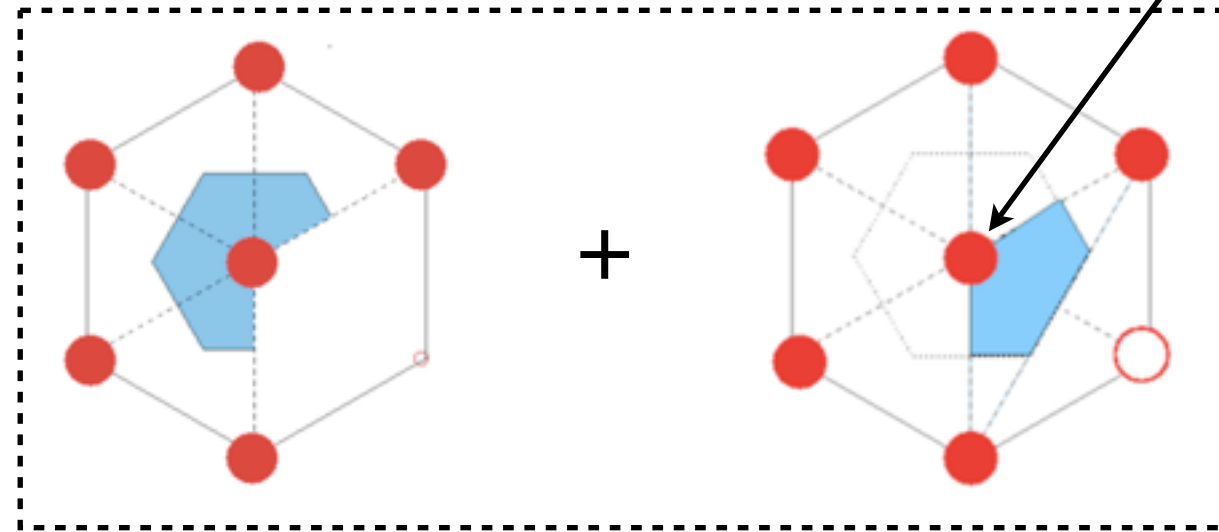
- Inclined sample provides about $\sim 30\%$ of extra sky coverage
- This extra coverage is very important to many of the analyses to be discussed here

General note on Auger SD data samples - II

6T5 (tight trigger)



5T5-pos+ (relaxed trigger)



Hottest and/or closest to the core station

Core inside equilateral

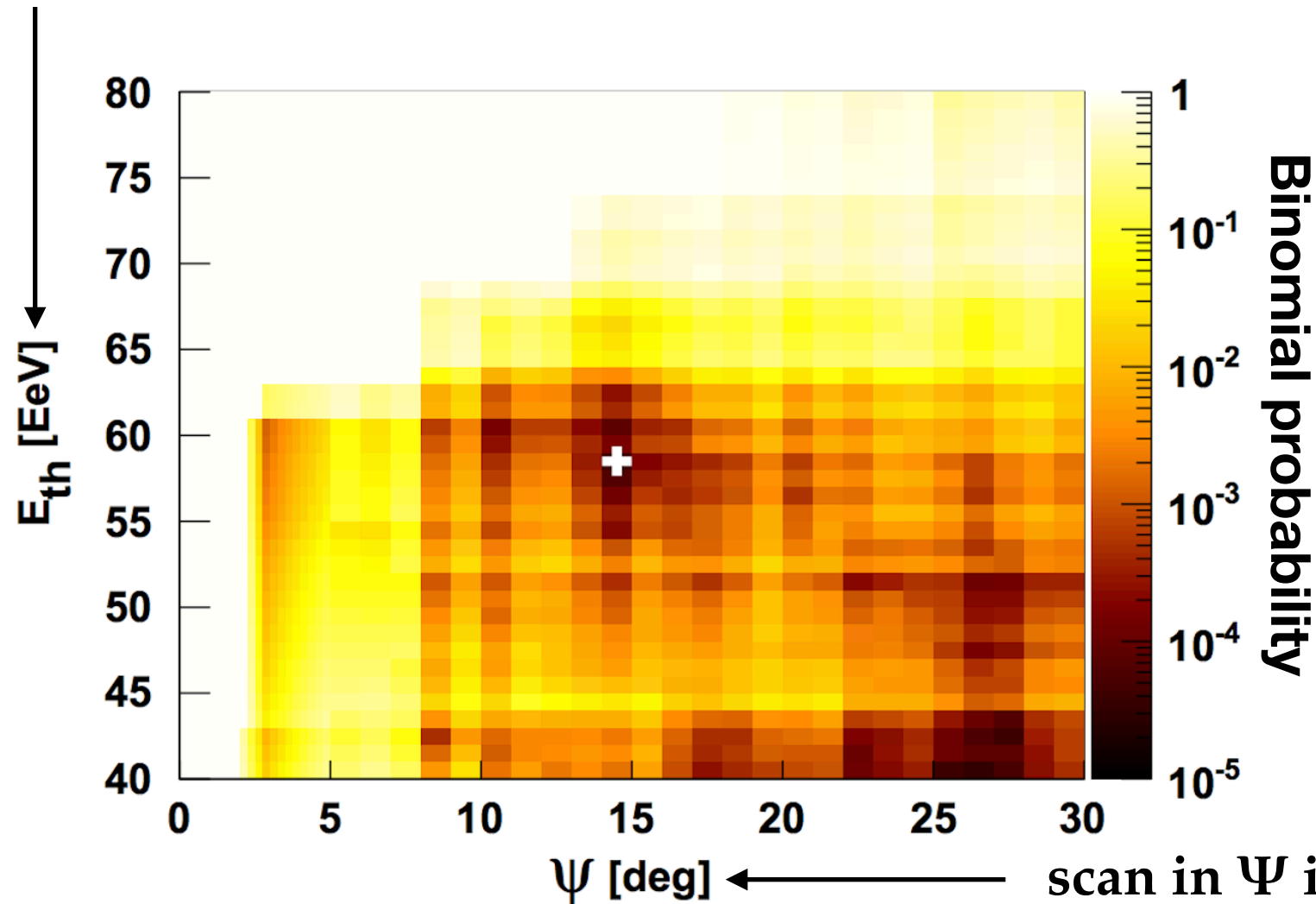
Core inside isosceles

- **6T5**: all 6 stations in the first crown active at the moment the event is detected
- **5T5-pos+**: 5 stations in the first crown active at the moment the event is detected, and core falls either inside an equilateral or an isosceles triangle
- Checked that reconstruction is not biased by including this events
- Important extra statistics! : $5T5\text{-pos+} / 6T5 \sim 18\%$

Small to intermediate scale anisotropies

Centaurus A

scan in E_{th} in 1 EeV steps



Minimum probability found at:

$$E_{th} = 58 \text{ EeV}, \Psi = 15^\circ$$

$$n_{obs} = 19, n_{exp} = 6.0$$

$$P \sim 1.1 \times 10^{-5}$$

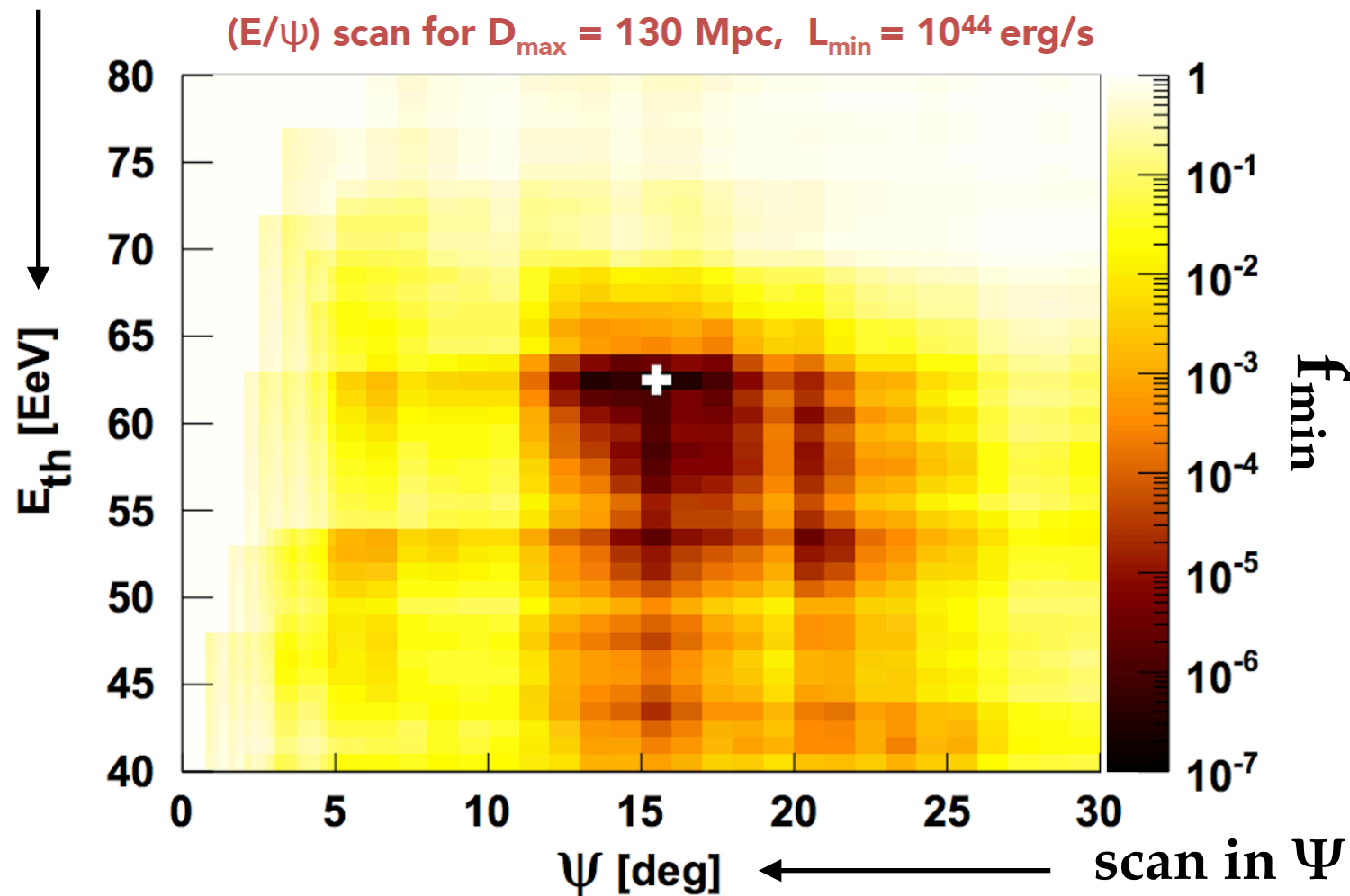
Post-trial (E_{th}, Ψ):

$$\sim 1.1 \times 10^{-3}$$

- Get the cumulative number of events for a given energy threshold (E_{th}) and angular window (Ψ) around CenA for data (n_{obs})
- Estimate the average number of events inside the same angular window from simulations (n_{exp})
- Compute binomial probability P of measuring n_{obs} given n_{exp}
- Penalize for scan in energy threshold and angular window (post-trial prob.)

Bright AGNs from Swift-BAT catalog

scan in E_{th} in 1 EeV steps



Minimum probability found at:

$$E_{\text{th}} = 62 \text{ EeV}, \Psi = 16^\circ$$

$$n_{\text{obs}} = 57, n_{\text{exp}} = 26.4$$

$$f_{\text{min}} = 1 \times 10^{-7}$$

Post-trial ($E_{\text{th}}, \Psi, L_{\text{min}}, D_{\text{max}}$):

$$\sim 6.5 \times 10^{-4}$$

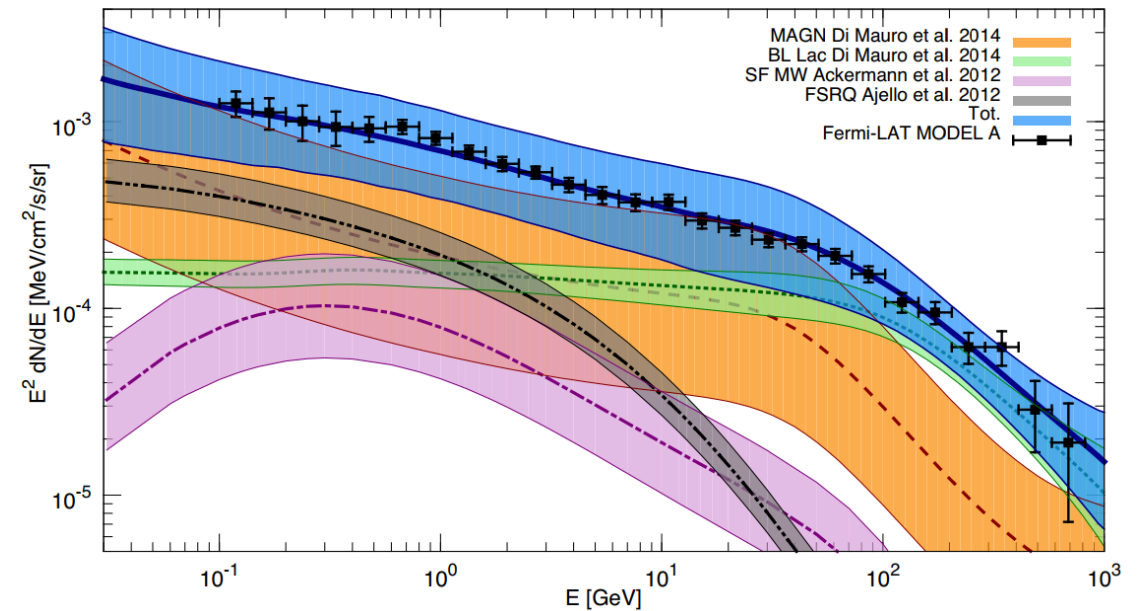
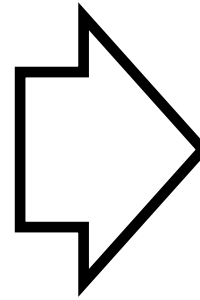
- Get the cumulative number of pairs for a given energy threshold (E_{th}) and angular distance (Ψ) wrt to catalog objects (n_{obs})
- Estimate the fraction of isotropic simulations (f_{min}) with number of pairs as large as in the data
- Penalize for scan in energy threshold, angular window, minimum luminosity of source and maximum distance (post-trial prob.)

Selection of extragalactic gamma-ray sources

Di Mauro & Donato, PRD 91 (2015) 123001

EGB composition with MW SF model

AGNs and starburst galaxies dominate the x-gal γ -ray background



Active Galactic Nuclei:

- Fermi 2FHL catalog
- $\Phi(>50 \text{ GeV})$ as proxy for UHECR flux
- 17 objects up to 250 Mpc
- Most blazars and BL-Lac type

Starburst galaxies:

- Fermi-LAT list of star-formation objects (Ackermann+12)
- $\Phi(>1.54 \text{ GHz})$ as proxy for UHECR flux
- Brightest objects selected: $\Phi(>1.54 \text{ GHz}) > 0.3 \text{ Jy}$
- 23 objects in final sample

Assumption: UHECR flux is correlated to the non-thermal photon flux

Unbinned likelihood:

exposure



$$\mathbf{L} = \prod_{i=1}^N [\omega(\hat{\mathbf{n}}_i) \times \text{model}(\hat{\mathbf{n}}_i)]$$



$$\alpha \times \text{sources} + (1 - \alpha) \times \text{isotropy} \otimes \text{Gaussian}(\theta)$$



Include weights to account for flux attenuation (especially important for AGNs)

2D parameter space (α, θ) :

α : Anisotropic fraction

θ : RMS deflection

Scan in energy threshold [20:80] EeV in steps of 1 EeV

Test statistics (TS) is a log-likelihood ratio of two hypotheses:

$$\text{TS} = 2 \ln \left(\frac{H_1}{H_0} \right)$$

\leftarrow
 \leftarrow

AGN or starburst as sources

Isotropy

TS vs threshold energy

Starburst Galaxies

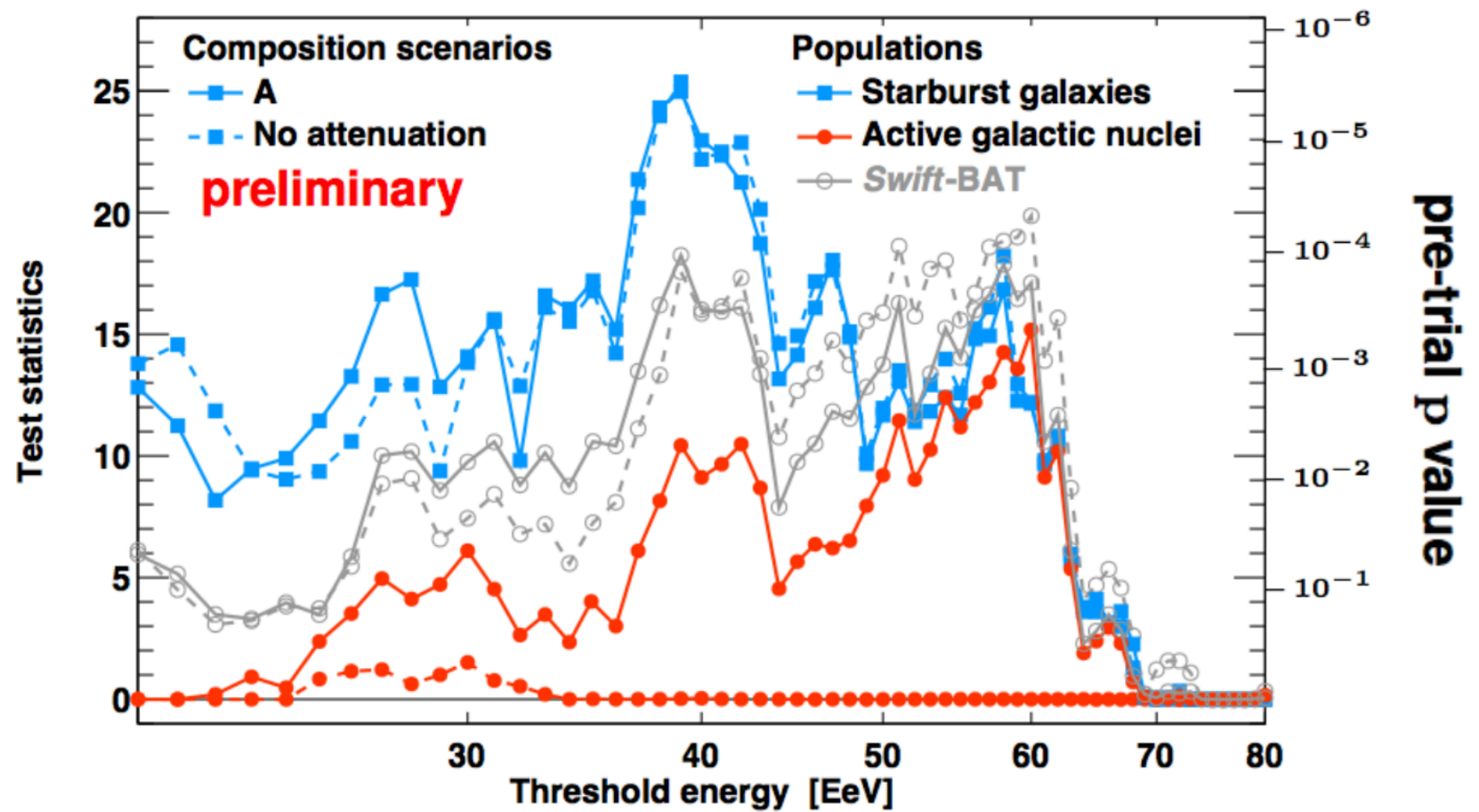
TS = 24.9, $E_{th} = 39$ EeV

γ -ray detected AGNs

TS = 15.2, $E_{th} = 60$ EeV

Swift-BAT AGNs

TS = 19.9, $E_{th} = 60$ EeV



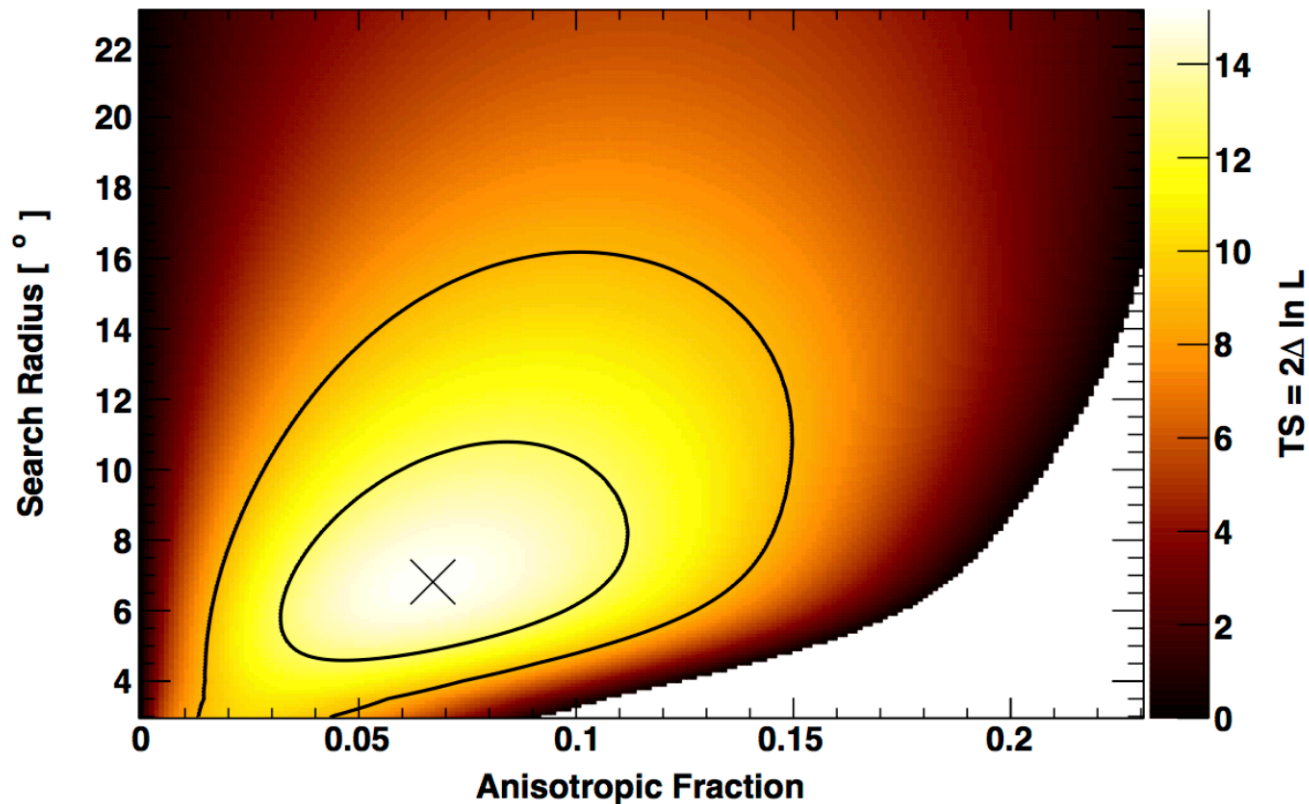
- Flux attenuation weights very important for AGNs, but negligible for starburst (nearby)
- Weights, however, depend strongly on the mass composition scenario

Mass composition scenario:

- Combined spectrum+ X_{max} fit
- EPOS-LHC as hadronic model
- Uniform source distribution

| Element | Fraction |
|---------|----------|
| H | 0% |
| He | 67.3% |
| N | 28.1% |
| Si | 4.6% |
| Fe | 0% |

Active galactic nuclei - $E > 60$ EeV



$$\alpha = 7\%, \theta = 7^\circ$$

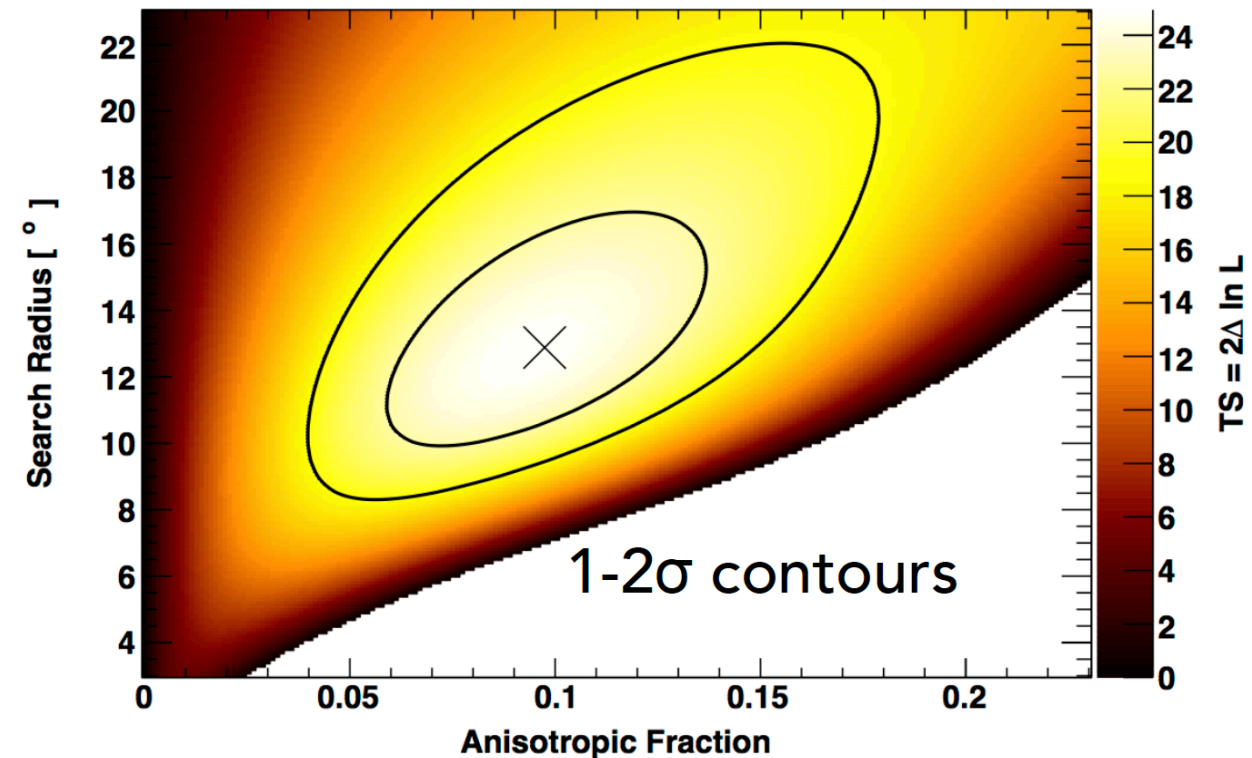
$$\text{TS} = 15.2$$

$$E_{\text{th}} = 60 \text{ EeV}$$

$$\text{Pre-trial: } 5 \times 10^{-4}$$

$$\text{Post-trial: } 3 \times 10^{-3} (2.7\sigma)$$

Starburst galaxies - $E > 39$ EeV



$$\alpha = 10\%, \theta = 13^\circ$$

$$\text{TS} = 24.9$$

$$E_{\text{th}} = 39 \text{ EeV}$$

$$\text{Pre-trial: } 4 \times 10^{-6}$$

$$\text{Post-trial: } 4 \times 10^{-5} (3.9\sigma)$$

- Post-trial prob. = fraction of isotropic simulations with TS greater than in data while scanning across the same energy bins
- Previous searches and hidden trials not account for

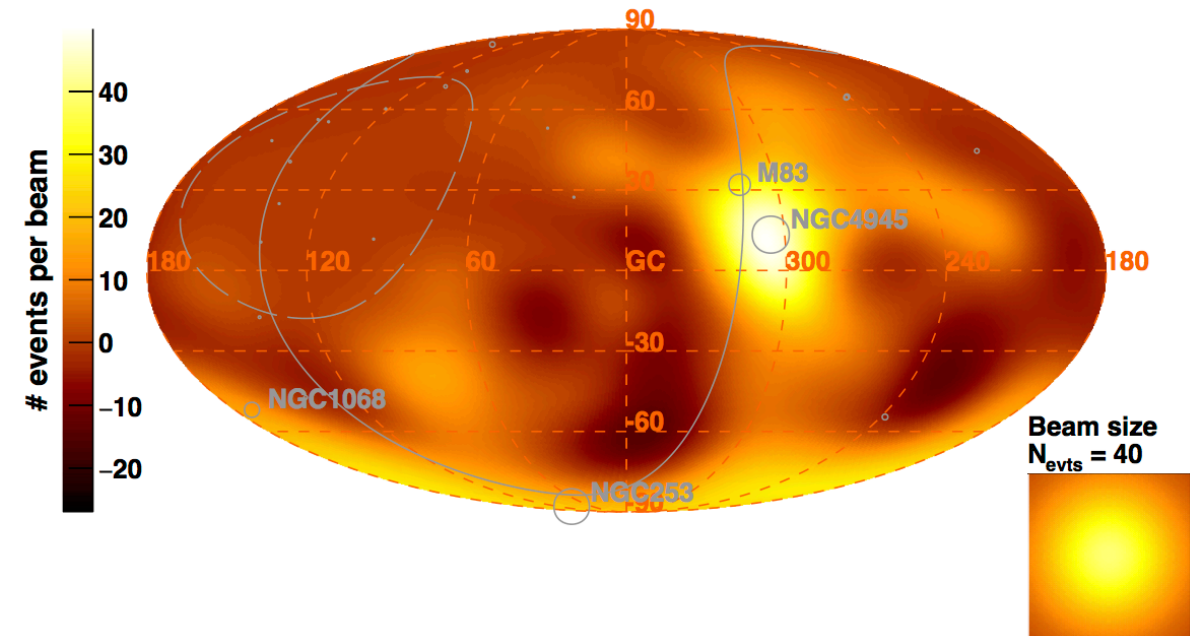
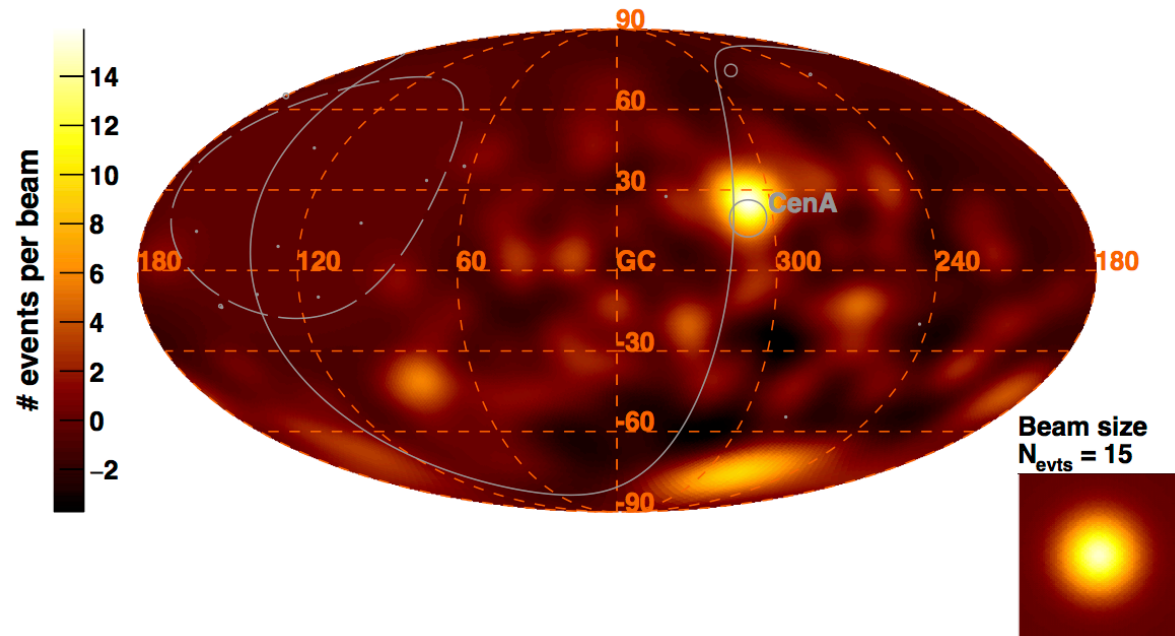
Best-fit maps (galactic coord.)

γ -ray AGNs

Starburst galaxies

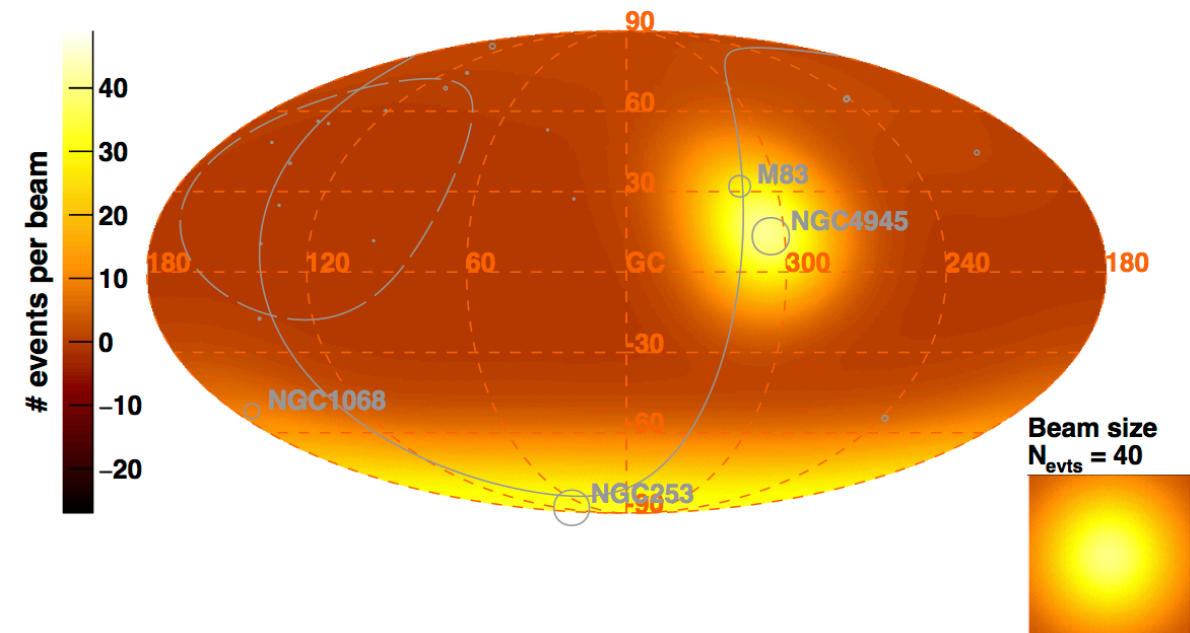
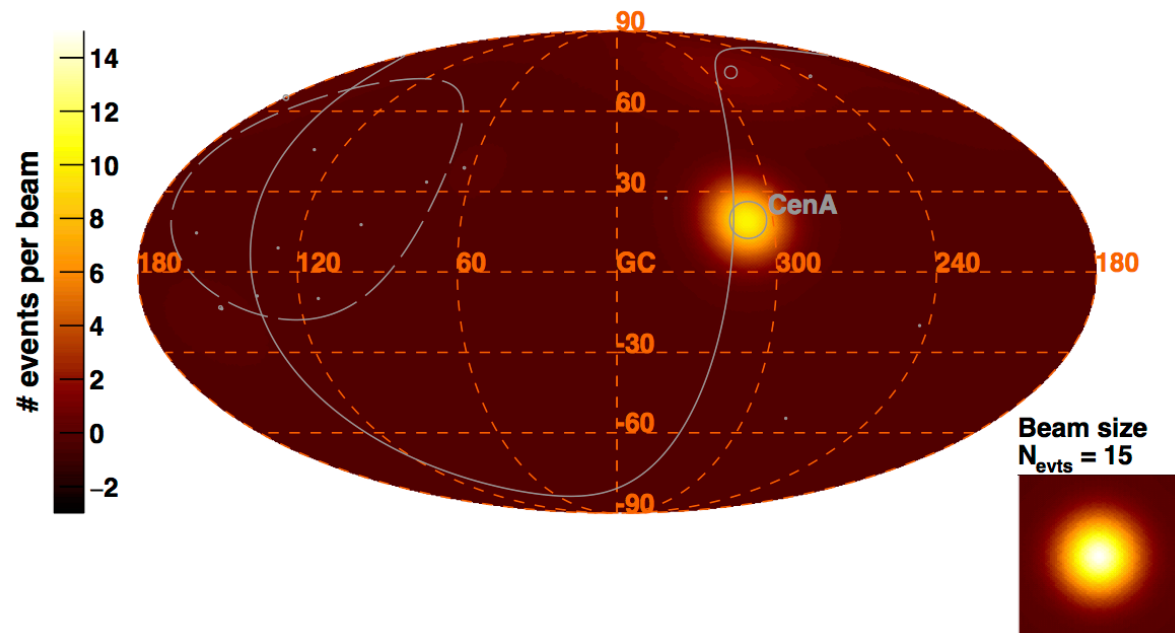
Observed Excess Map - $E > 60$ EeV

Observed Excess Map - $E > 39$ EeV



Model Excess Map - $E > 60$ EeV

Model Excess Map - $E > 39$ EeV

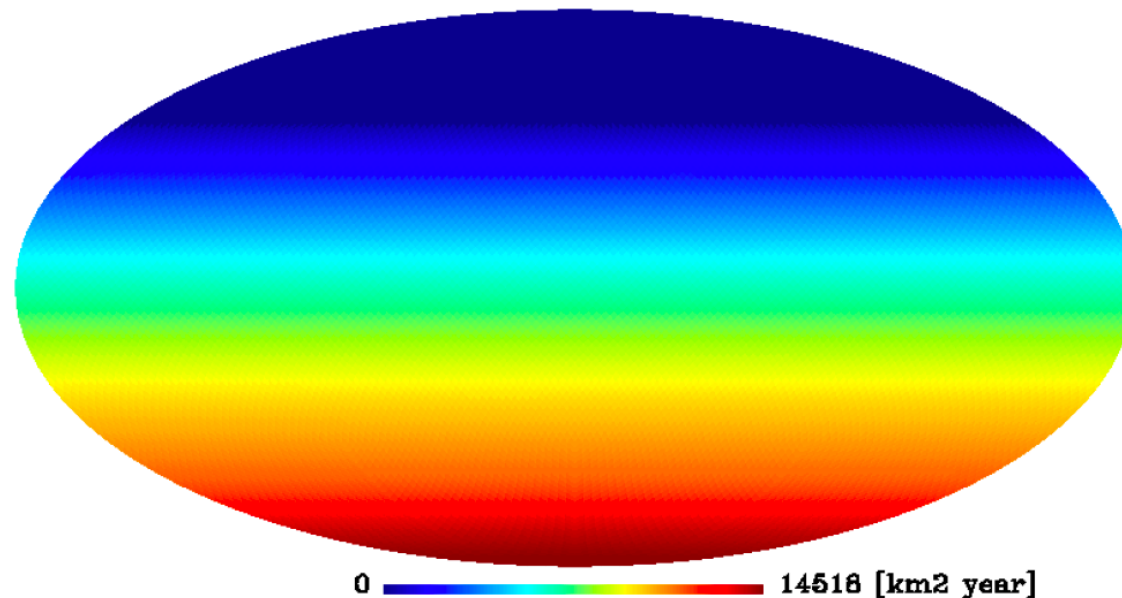


Large scale anisotropies

Dipole above 8 EeV - dataset

- Period: 01-01-2004 to 08-31-2016
- Additional sky coverage ($\sim 30\%$) provided by inclined events ($60^\circ < \theta < 80^\circ$)
- Enhanced statistics with the use of relaxed (but high quality) triggers
- Two major systematic effects understood and corrected:
 - Weather (temperature and pressure) induced modulations
 - Distortions on ground level muon density by the geomagnetic field
- Total integrated exposure of 76,800 km² sr year

Directional exposure



Dipole detection

Science 57 (2017) 1266

Analysis of first harmonic modulation in RA and azimuth

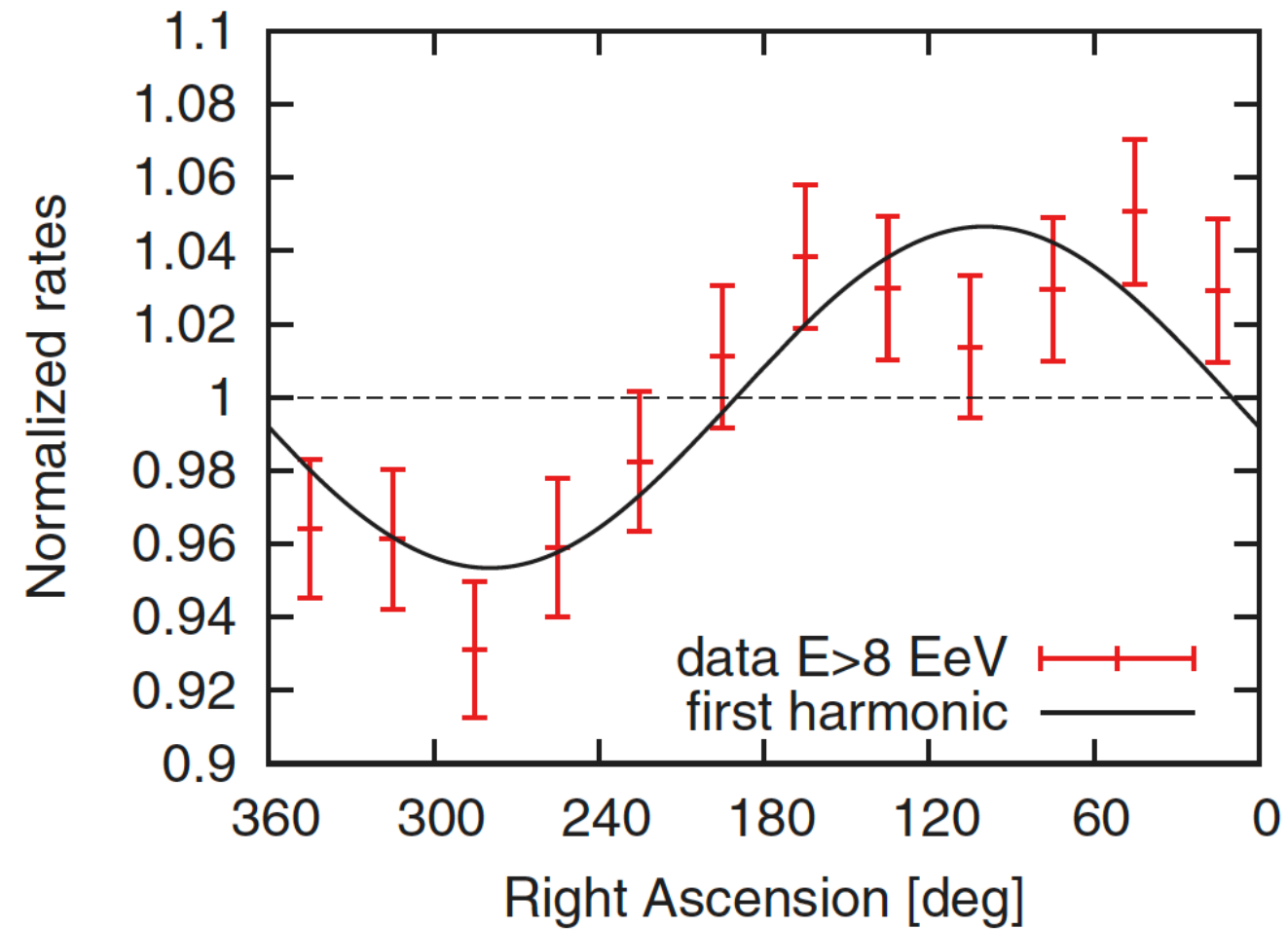
$$a_\alpha = \frac{2}{\mathcal{N}} \sum_{i=1}^N w_i \cos \alpha_i$$

Account for non-uniformities of the exposure in RA and a slight tilt of the array

$$b_\alpha = \frac{2}{\mathcal{N}} \sum_{i=1}^N w_i \sin \alpha_i$$

Amplitude and phase of modulation

$$r_\alpha = \sqrt{a_\alpha^2 + b_\alpha^2} \quad \tan \varphi_\alpha = \frac{b_\alpha}{a_\alpha}$$



| Energy (EeV) | Number of events | Fourier coefficient a_α | Fourier coefficient b_α | Amplitude r_α | Phase φ_α ($^\circ$) | Probability $P(\geq r_\alpha)$ |
|--------------|------------------|--------------------------------|--------------------------------|---------------------------|-------------------------------------|--------------------------------|
| 4 to 8 | 81,701 | 0.001 ± 0.005 | 0.005 ± 0.005 | $0.005^{+0.006}_{-0.002}$ | 80 ± 60 | 0.60 |
| ≥ 8 | 32,187 | -0.008 ± 0.008 | 0.046 ± 0.008 | $0.047^{+0.008}_{-0.007}$ | 100 ± 10 | 2.6×10^{-8} |

- 5.6 σ pre-trial signal
- 5.2 σ post-trial (penalized for scan in 2 energy bin)

pre-trial probability:

$$P(\geq r_\alpha) = \exp\left(-\frac{N r_\alpha^2}{4}\right)$$

Dipole reconstruction

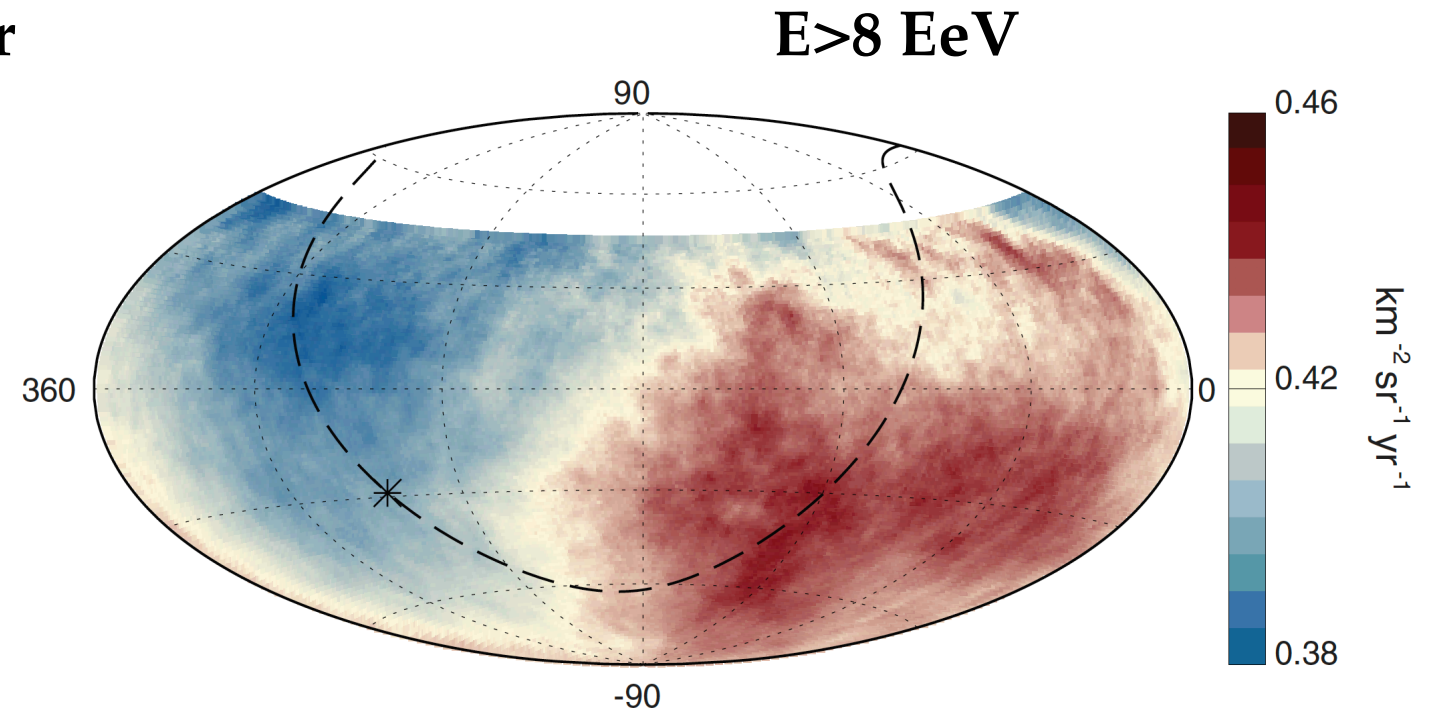
Science 57 (2017) 1266

Components parallel and perpendicular to the Earth rotation axis:

$$d_z \approx \frac{b_\varphi}{\cos \ell_{\text{obs}} \langle \sin \theta \rangle} \quad d_\perp \approx \frac{r_\alpha}{\langle \cos \delta \rangle}$$

Right ascension and declination:

$$\alpha_d = \varphi_\alpha \quad \tan \delta_d = \frac{d_z}{d_\perp}$$

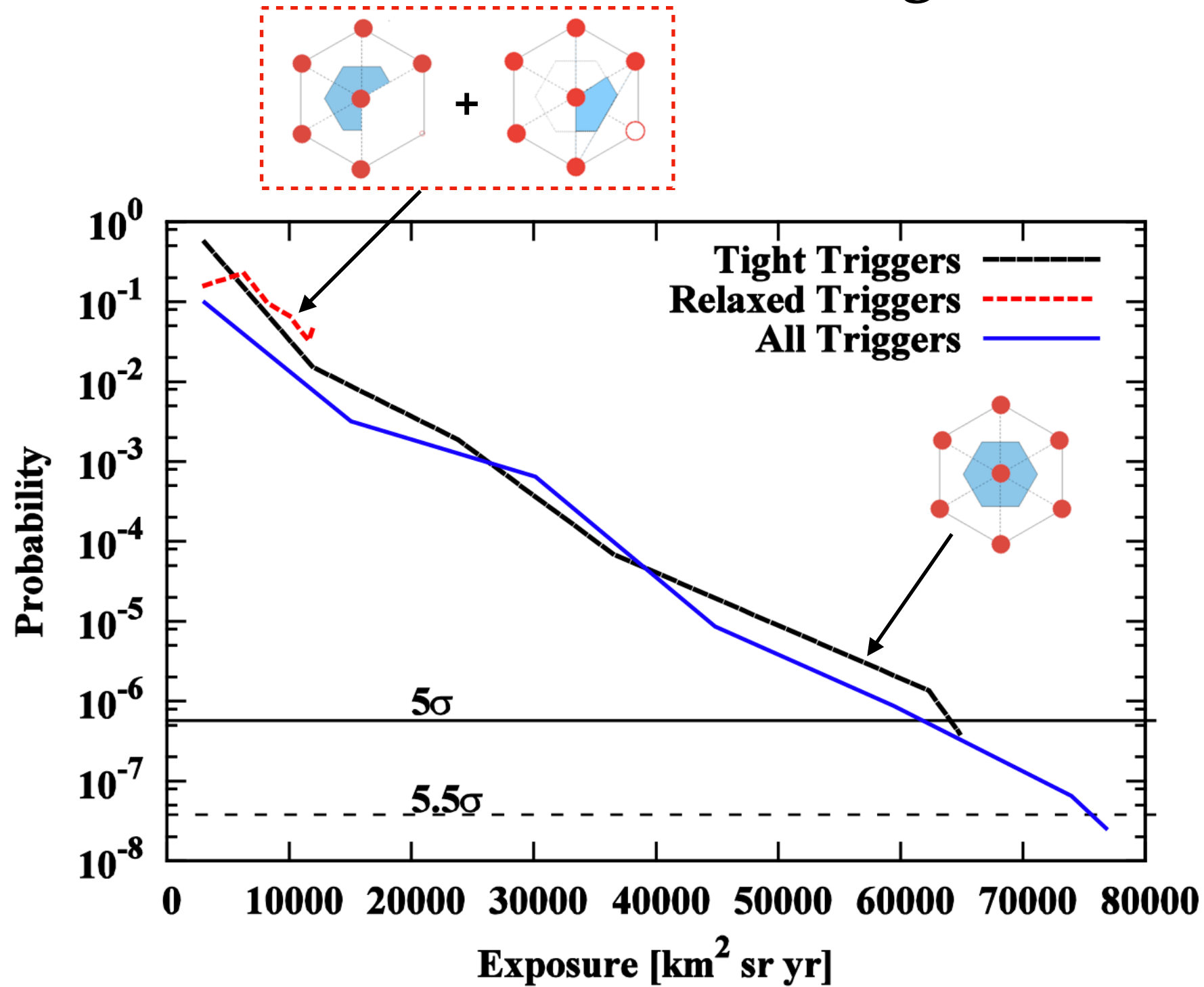


| Energy (EeV) | Dipole component d_z | Dipole component d_\perp | Dipole amplitude d | Dipole declination δ_d (°) | Dipole right ascension α_d (°) |
|--------------|------------------------|----------------------------|---------------------------|-----------------------------------|---------------------------------------|
| 4 to 8 | -0.024 ± 0.009 | $0.006^{+0.007}_{-0.003}$ | $0.025^{+0.010}_{-0.007}$ | -75^{+17}_{-8} | 80 ± 60 |
| ≥ 8 | -0.026 ± 0.015 | $0.060^{+0.011}_{-0.010}$ | $0.065^{+0.013}_{-0.009}$ | -24^{+12}_{-13} | 100 ± 10 |

- Reconstruction assumes the dipole is the dominant component of the anisotropy
- Analysis of the power spectrum gives support to this hypothesis

Time evolution of the signal

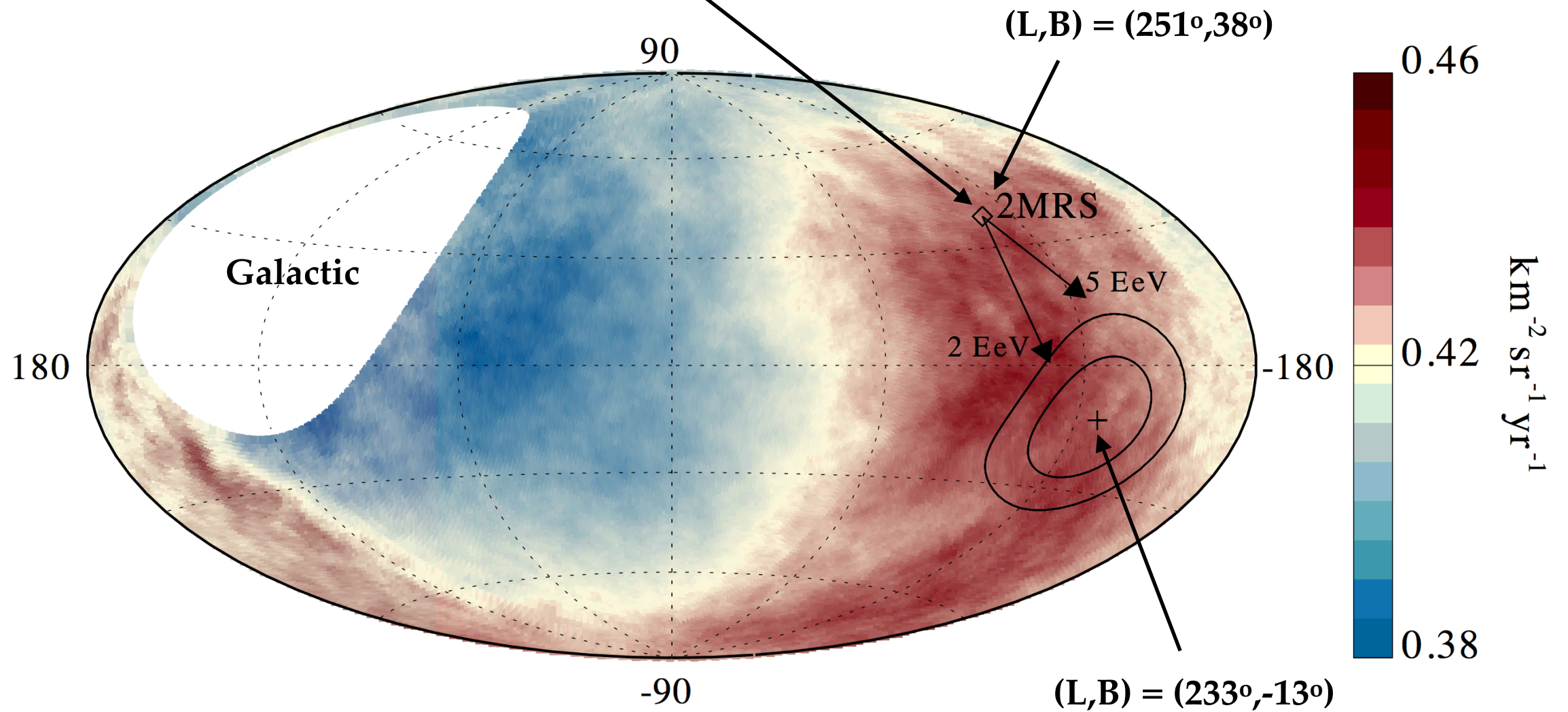
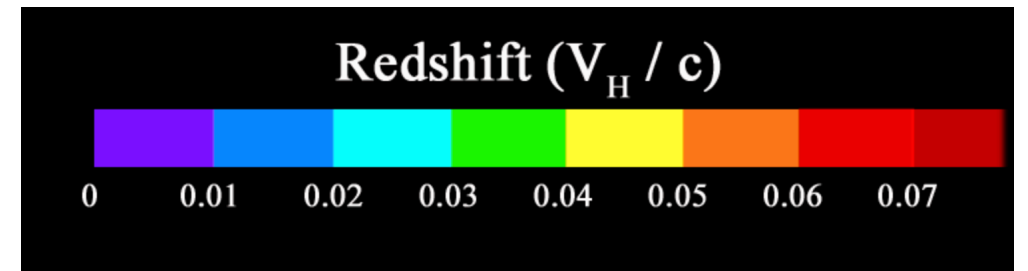
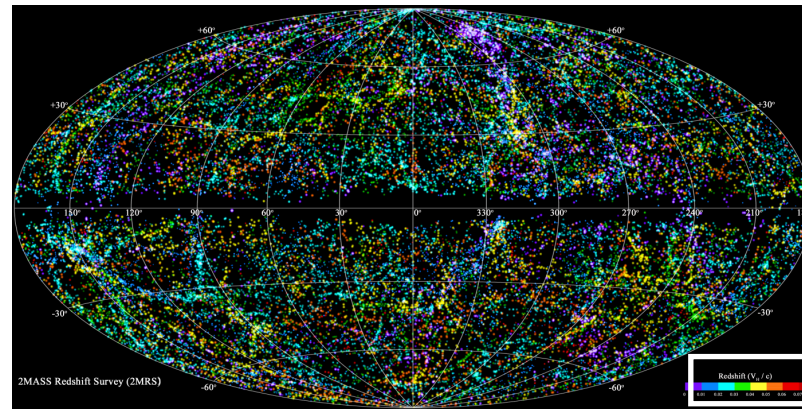
Science 57 (2017) 1266



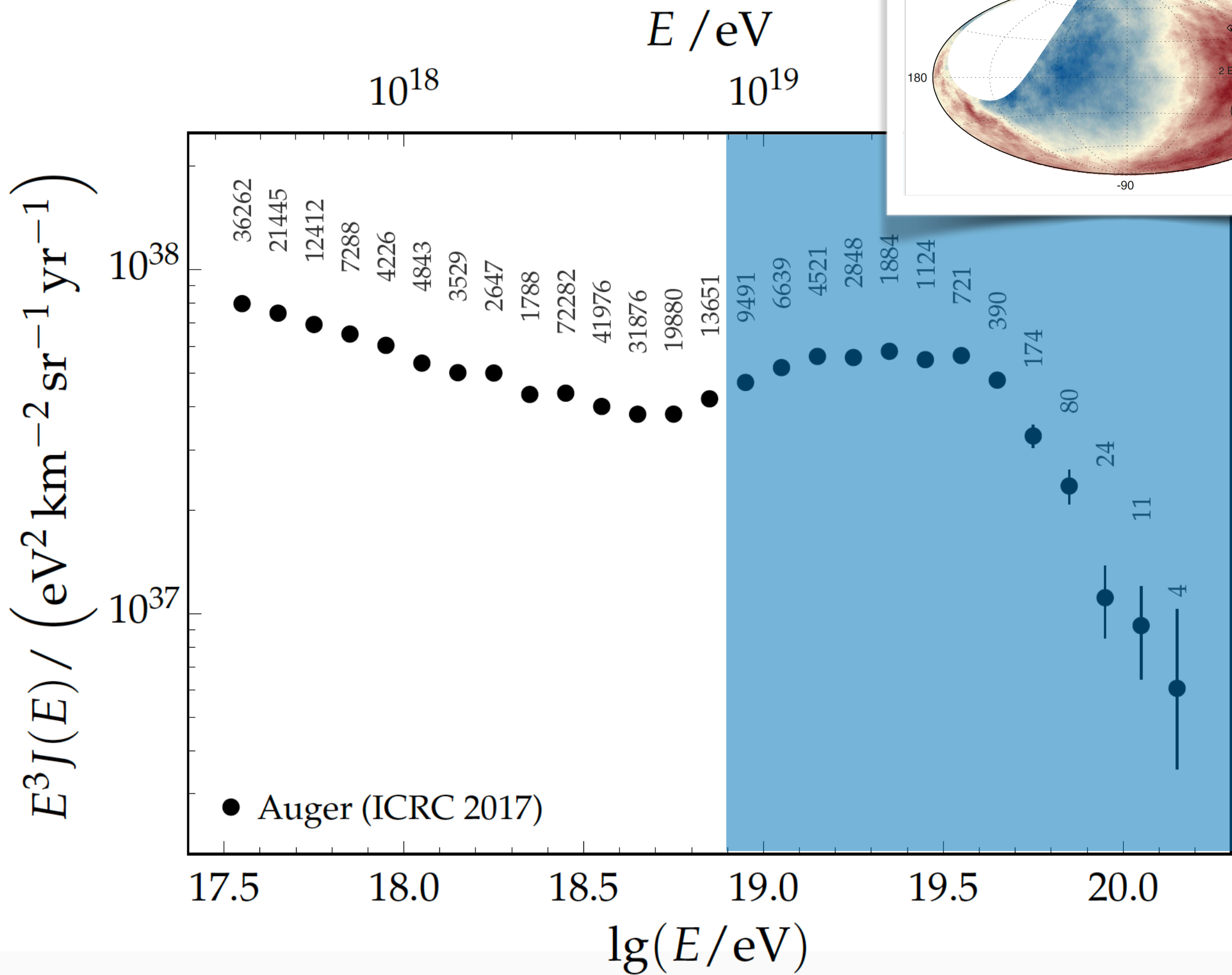
- Steady drop of the chance probability as data is accumulated



2MASS Redshift Survey (2MRS)



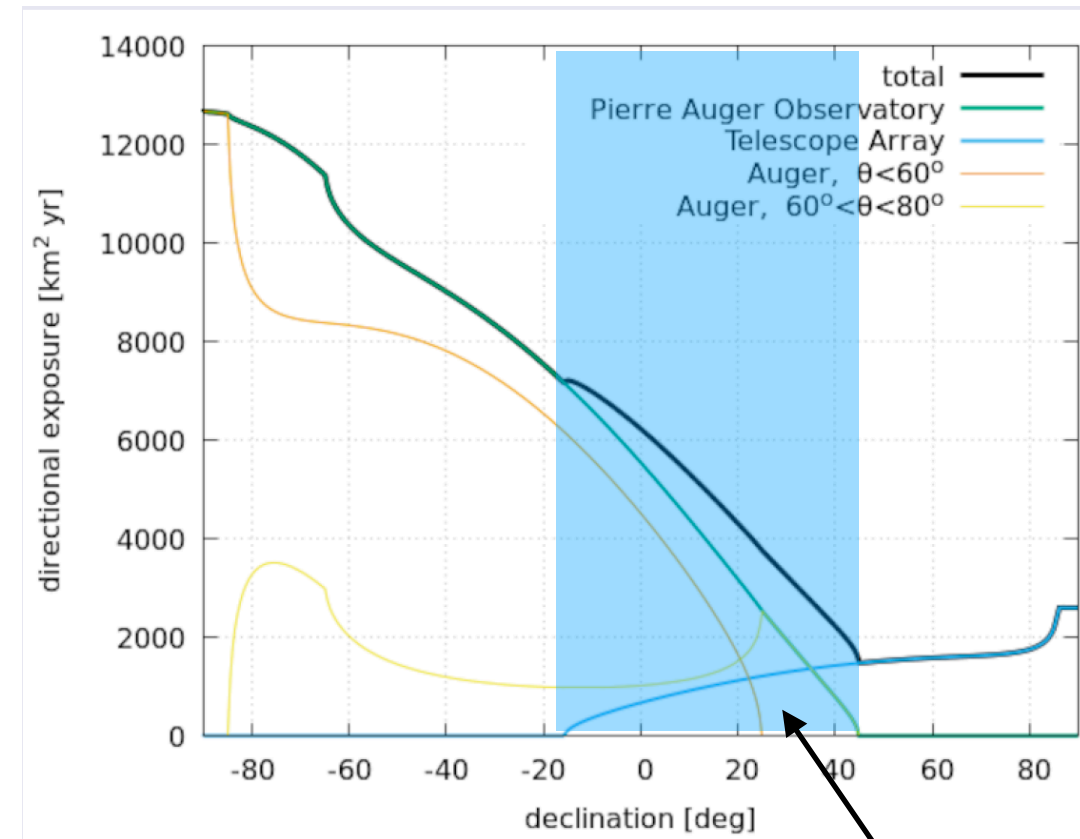
Typically, 5-20% dipole amplitudes can be obtained from local inhomogeneities and diffusion through magnetic fields depending on CR composition



Combined full sky analyses

| TA | Auger |
|----------------------------|-----------------------------|
| $\theta < 55$ deg. | $\theta < 80$ deg. |
| 8700 km ² sr yr | 66452 km ² sr yr |
| $E > 57$ EeV | $E > 40$ EeV |
| 83 events | 602 events |

- Twice as many events as in ApJ 794 (172) 2014
- Found E_{Auger} and E_{TA} for which the integrated fluxes match:



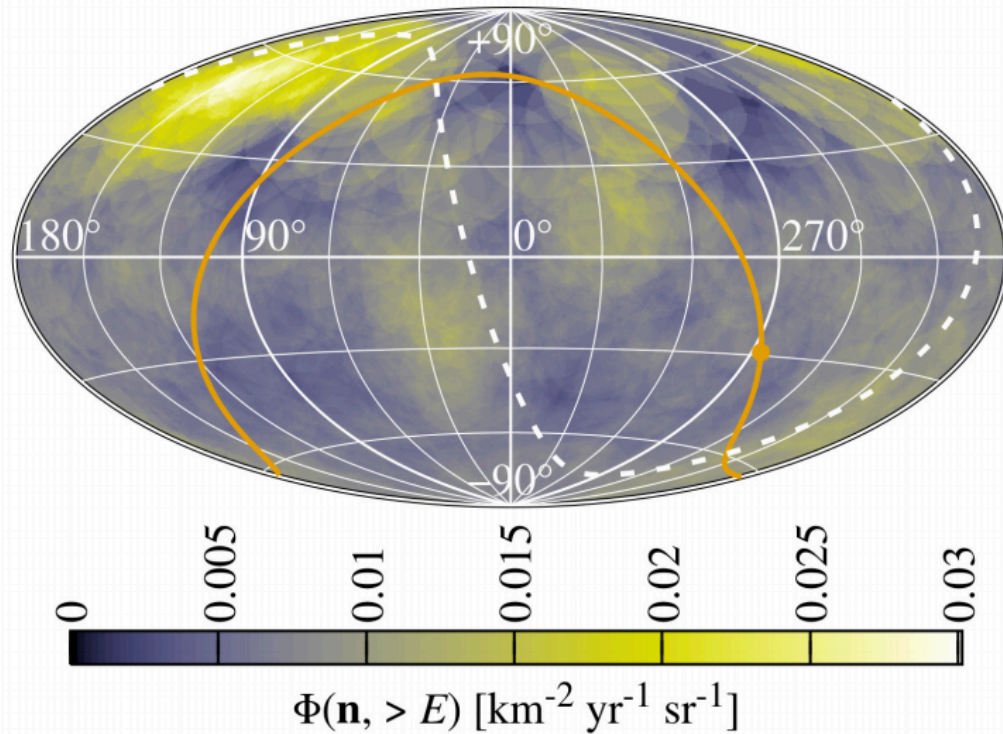
$$\sum_{\text{events in band}} \frac{1}{\omega(\mathbf{n}_i)} \quad \leftarrow \quad \text{Unbiased flux estimator}$$

Common band: [-16,+45]
Fiducial band: [-12,+42]

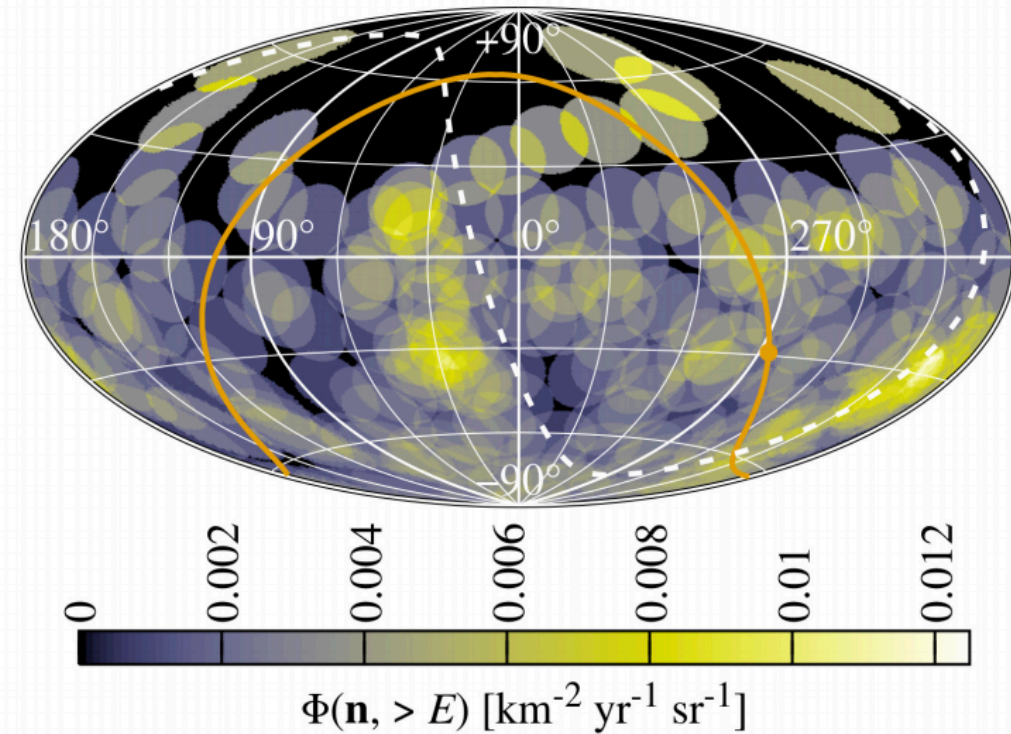
| reference flux km ⁻² yr ⁻¹ | E_{Auger} EeV | E_{TA} EeV | flux stat. uncertainty Auger | flux stat. uncertainty TA | motivation |
|---|---------------------------|------------------------|---------------------------------|------------------------------|----------------|
| 0.042 | 42 ± 1 | 57 ± 4 | 9% | 16% | TA 2014 [4] |
| 0.013 | 54 ± 1 | 89^{+4}_{-17} | 14% | 29% | Auger 2015 [5] |

Combined flux sky map (equatorial)

$E_{TA} > 57 \text{ EeV} / E_{Auger} > 42 \text{ EeV}$, 20° -radius window

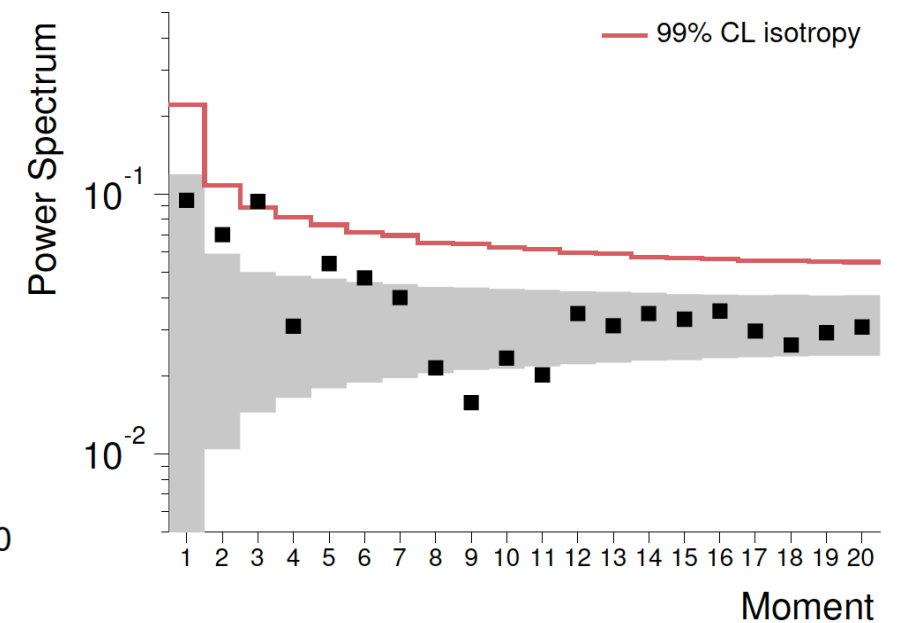
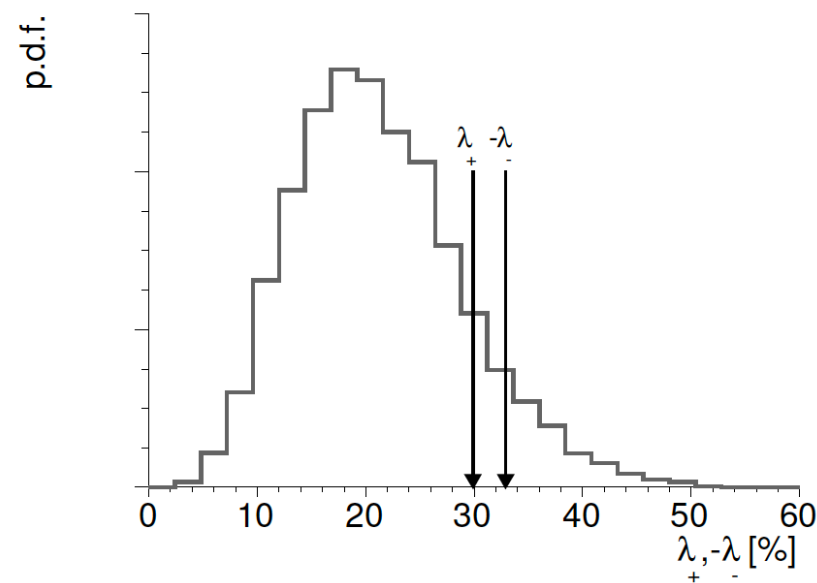
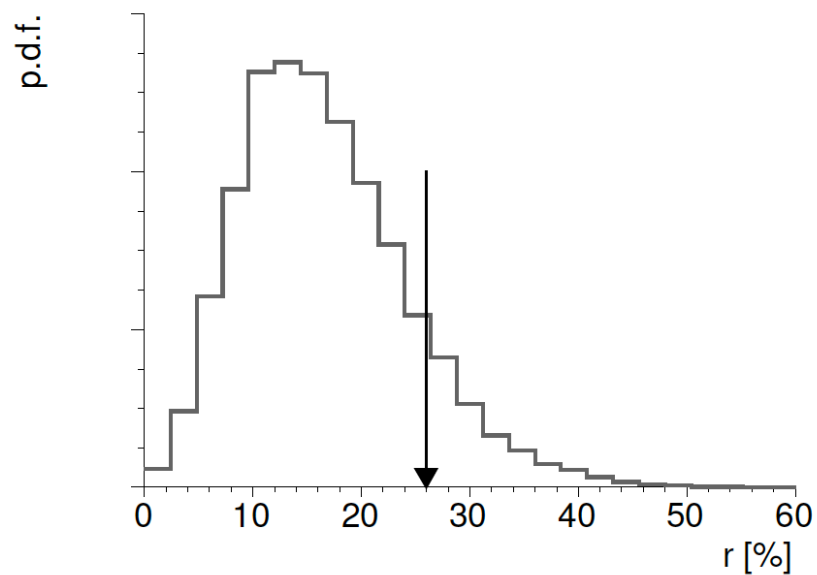


$E_{TA} > 89 \text{ EeV} / E_{Auger} > 54 \text{ EeV}$, 12° -radius window



$$\Phi(\mathbf{n}) = \frac{\Phi_0}{4\pi} (1 + r\mathbf{d} \cdot \mathbf{n} + \lambda_+(\mathbf{q}_+ \cdot \mathbf{n})^2 + \lambda_0(\mathbf{q}_0 \cdot \mathbf{n})^2 + \lambda_-(\mathbf{q}_- \cdot \mathbf{n})^2 + \dots)$$

Compatibility with isotropy



Summary

- **Anisotropy searches performed at all angular scales: small, intermediate and large**
- **Indications of anisotropy at the 4σ level from a maximum log-likelihood analysis based on starburst galaxy model**
- **Observation of a dipolar large scale pattern at more than 5σ level above 8 EeV**
- **Direction of the dipole ($\sim 120^\circ$ away from GC) is inconsistent with a galactic origin for the bulk of this UHECRs**
- **Full sky coverage achieved with combined Auger-TA flux sky maps at high energy thresholds (no significant anisotropy seen so far)**

